RSC Advances

ROYAL SOCIETY OF CHEMISTRY

www.rsc.org/advances

Journal Name

RSCPublishing

ARTICLE

Spectroscopic study of a synthesized Alq_3 end-capped oligothiophene applied in organic solar cells

Cite this: DOI: 10.1039/xoxxooooox

Venla M. Manninen,*[a] Juha P. Heiskanen,[b] Kimmo M. Kaunisto,[a] Osmo E. O. Hormi[b] and Helge J. Lemmetyinen[a]

Received ooth January 2012,
Accepted ooth January 2012

DOI: 10.1039/xoxxooooox

www.rsc.org/

In this paper, we report the spectroscopic properties of a synthetically tailored Alq_3 end-capped oligothiophene ($(Alq_3)_2$-OT) studied by steady state and time resolved spectroscopic methods in chloroform and solid films. In chloroform a photo-induced intramolecular electron transfer from the oligothiophene backbone to the Alq_3 moiety was observed. When $(Alq_3)_2$-OT was mixed with a fullerene derivative (PCBM) in chloroform, we demonstrate that $(Alq_3)_2$-OT donates an electron to PCBM. With that in mind, $(Alq_3)_2$-OT was applied as a dopant molecule to improve the efficiency of P3HT:PCBM bulk hetero junction (BHJ) solar cells.

Introduction

Growing interest in organic electronics, such as organic solar cells (OSCs) and organic light emitting diodes (OLEDs), has increased the need to synthesize new organic materials that can be applied in producing low-cost and light weight devices. Detailed understanding of molecular properties and inter- or intramolecular interactions is a prerequisite for developing new photoactive and functional materials. In recent years, solution-processable small molecule donor materials have gained increasing amounts of attention in solar cell research. Small molecule materials have several advantages over polymers including well-defined structures and easier purification.

A large number of small-molecule compounds used in organic electronic devices utilize thiophene units as components of their chemical structure. Thiophene containing compounds have been used as photoactive donor molecules and hole transporting materials in OSCs that show good photovoltaic performance.[1] Thiophene also plays an important role in many organic dyes used in dye-sensitized solar cells by acting as a π-conjugation bridge.[2]

Tris-(8-hydroxyquinoline)aluminum (Alq_3) complex has widely been used as light-emitting and electron transporting material in OLEDs, since its electroluminescence properties were discovered by Tang and VanSlyke.[3] After that, the electron mobility of Alq_3 has been extensively studied[4] and it has been used as an electron transporting buffer layer in conventional organic solar cells to increase the stability and lifetime of the cells.[5]

Recently, various Alq_3 derivatives with tailored energy levels exhibited up to a 30 % increase in the efficiency of the inverted cell compared to those with the parent Alq_3 as a hole-transporting anode buffer layer.[6] Furthermore, Alq_3 and its derivatives have been used as dopants in the photoactive layer of OSCs, which increased the efficiency of the cells remarkably.[6a]

In this paper, we present the synthesis of Alq_3 end-capped oligothiophene ($(Alq_3)_2$-OT) and extensively study its spectroscopic properties. Fluorescence properties of $(Alq_3)_2$-OT differ drastically from those of the parent Alq_3 complex and the thiophene oligomer. We concentrate on understanding the properties of the synthesized molecule by steady state and time-resolved spectroscopic methods. The spectroscopic measurements strongly support an intramolecular electron transfer from the oligothiophene backbone to the Alq_3 complex.

Interaction of the $(Alq_3)_2$-OT with PCBM was also studied. Based on those results, we propose that $(Alq_3)_2$-OT can donate an electron to PCBM. With that in mind, $(Alq_3)_2$-OT was tested as a dopant molecule in the P3HT:PCBM layer of the bulk hetero junction (BHJ) for improving cell efficiency. Previous reports have suggested that the cell efficiency was increased due to improved morphology, crystallization, and charge transport caused by doping with Alq_3 molecules.[6a] Here we propose that $(Alq_3)_2$-OT can function in the BHJ active layer as an additional light-absorber and donate electrons to PCBM, thereby improving the cell efficiency.

The hole transporting properties of $(Alq_3)_2$-OT were also tested by using it as a buffer layer in inverted OSCs. The improved cell efficiencies and stabilities measured several weeks after the cell preparation demonstrate that the

compatibility of the parent Alq_3 with BHJ materials and its charge transporting properties can be improved by combining the complexes with the oligothiophene structure.

Results and discussion

Synthesis of $(Alq_3)_2$-OT. Commercially available starting material, compound **1**, was brominated with N-bromosuccinimide (NBS) to afford 5,5'''-dibromo-3,3'''-dihexyl-2,2':5',2'':5'',2'''-quaterthiophene (**2**) (Scheme 1). Compound **2** has been previously prepared by time intensive methods with various yields (50–92 %).[7] Our method applies the recent observation that thiophenes can be brominated neatly with NBS by using ultrasound irradiation and a suitable solvent.[8] After 1 h of reaction time and chromatographic purification, compound **2** could be collected in high yield (91 %). Ultrasound has previously been utilized together with NBS in bromination reactions of phenyl and naphthalene backbones.[9] In the best case, ultrasound irradiation offers a way to produce the desired bromination product efficiently: fast and facilely with a high yield and selectivity in mild conditions.

The literature provides one preparation method to produce 3,3''',3''''',4'-tetrahexyl-2,2':5',2'':5'',2''':5''',2''''':5''''',2''''''-sexithiophene (**3**).[7c] Nickel catalyzed coupling with Grignard reagent produced compound **3** in low yield (31%). In our hands, compound **3** was prepared and isolated in high yield (97 %) by applying Suzuki-Miayura cross-coupling approach.

Ultrasound assisted bromination could be also used to synthesize 5,5''''''-dibromo-3,3''',3''''',4'-tetrahexyl-2,2':5',2'':5'',2''':5''',2''''':5''''',2''''''-sexithiophene (**4**). Compound **4** was isolated in good yield (89%). The traditional method has previously given compound **4** in lower yield (77%).[7c]

Compound **5**, 5,5'-(3,3''',3''''',4'-tetrahexyl-2,2':5',2'':5'',2''':5''',2''''':5''''',2''''''-sexithiene-5,5''''''-diyl)bis[8-(benzyloxy)quinoline], can be synthesized by using two different methods. A traditional cross-coupling method, like Suzuki-Miayura used here, needs halogenated starting material (compound **4**) and a boronic acid derivative, (8-(benzyloxy)-5-(4,4,5,5-tetramethyl-1,3,2-dioxaborolan-2-yl)quinolone), to undergo coupling. The Suzuki-Miayura reaction gave compound **5** in good yield (85%). An alternative way to prepare compound **5** is to use the direct arylation method. Palladium

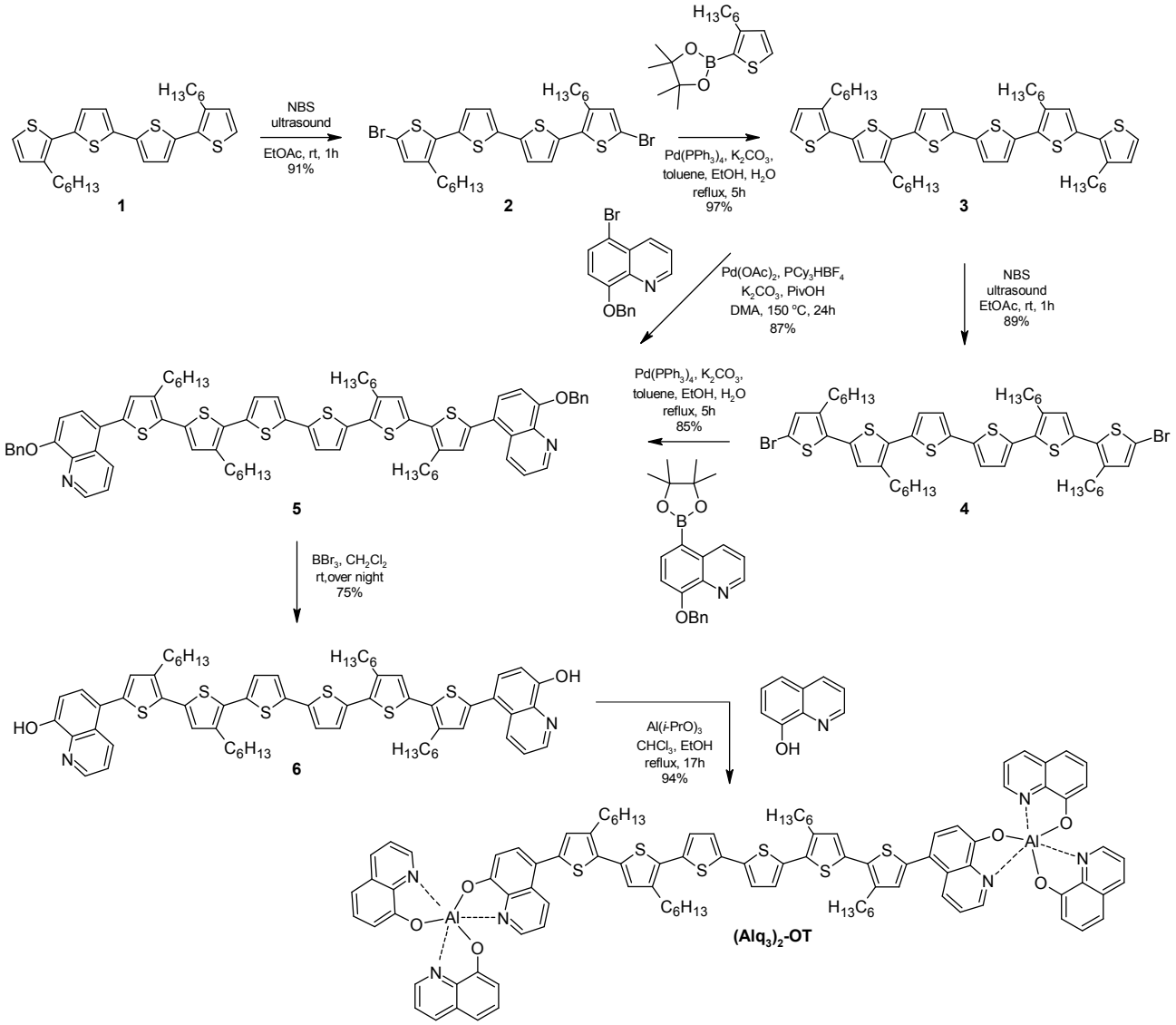

Scheme 1. Synthetic scheme of $(Alq_3)_2$-OT.

catalyzed direct arylation of thiophenes has recently shown potential as an efficient coupling reaction.[10] Indeed, the direct arylation method was shown to be a more convenient approach to produce compound **5**. Compound **3** underwent direct arylation smoothly with 8-(benzyloxy)-5-bromoquinoline to afford compound **5** in good yield (87%). In this way, two addiotional reaction steps of Suzuki-Miyaura reaction, bromination of compound **3** and borylation of 8-(benzyloxy)-5-bromoquinoline, can be avoided and the desired product **5** can be isolated using a simple filtration and washing procedure.

Removal of the benzyl protecting group was done with BBr_3 to afford 5,5'-(3,3'''',3''''',4'-tetrahexyl-2,2':5',2'':5'',2''':5''',2'''':5'''',2'''''-sexithiene-5,5''''''-diyl)diquinolin-8-ol (**6**) in good yield (75%). Complexation of compound **6** and fixed amount of 8-hydroxyquinoline ligands (4 equiv) with Al^{3+} was performed by using Al(*i*-PrO)$_3$ (2 equiv) as an aluminum source. Finally, the target compound $(Alq_3)_2$-OT was isolated in high yield (94%).

Spectroscopic and electrochemical analysis. Steady state and time-resolved absorption and fluorescence emission measurements were carried out in order to compare the properties of the $(Alq_3)_2$-OT, Alq_3, and the oligothiophene compound (**5**). Compound **5** and $(Alq_3)_2$-OT were studied in 0.22 mM $CHCl_3$ solutions, while Alq_3 in 0.44 mM $CHCl_3$ solution. These concentrations were used to allow easier comparison between the free Alq_3 complex and $(Alq_3)_2$-OT, where two complexes are bound to one oligothiophene backbone. Results of the spectroscopic measurements are collected in Table 1.

Table 1. Summary of the spectroscopic properties of compound **5**, $(Alq_3)_2$-OT and Alq_3. A_{405nm} and I_{PL} refer to absorbance at 405 nm and fluorescence intensity maxima. respectively.

Compound (conc. mM)	$\lambda_{abs,max}$ (nm)	$\lambda_{PL,max}$ (nm)	A_{405nm}	$I_{PL,max}$ (pure)	$I_{PL,max}$ (mixture)
5 (0.22)	423	545	1.46	4.9×10^7	3.4×10^7
$(Alq_3)_2$-OT (0.22)	427	604	0.98	2.7×10^6	1.7×10^6
Alq_3 (0.44)	388	528	0.42	1.9×10^7	6.1×10^6

Normalized steady state absorption and fluorescence emission spectra of compound **5**, $(Alq_3)_2$-OT, P3HT, and Alq_3 are presented in Figure 1a. The absorption of the $(Alq_3)_2$-OT is slightly red-shifted compared to that of compound **5**. The fluorescence properties of the compounds differ significantly. The emission band of the $(Alq_3)_2$-OT is remarkably broadened, red-shifted and significantly lower in intensity compared to that of compound **5.** Time correlated single photon counting (TCSPC) measurements showed that the decays of compound **5** and Alq_3 are clearly monoexponential, but $(Alq_3)_2$-OT has a biexponential decay (Figures 1b–c). The decay associated spectra (DAS) show that compound **5** has one component with a lifetime of 0.71 ns and the $(Alq_3)_2$-OT has two components with lifetimes of 0.40 ns and 14.0 ns (Figures 1d–e). Obviously, the longer lived component corresponds to the lifetime of Alq_3 moiety and the shorter one to the oligothiophene backbone of the $(Alq_3)_2$-OT.

The fluorescence intensity of $(Alq_3)_2$-OT is significantly lower compared to those of the free Alq_3 and compound **5** (Table 1). The reason for the decreased fluorescence is most likely an intramolecular charge transfer from the oligothiophene backbone to the Alq_3 moieties. To better understand the possible charge transfer in the molecule, the energy levels of the compounds shown in Figure 2 were measured by differential pulse voltammetry (DPV curves: See ESI, Figure S6). The LUMO level of $(Alq_3)_2$-OT corresponds to that of Alq_3 and the HOMO level of $(Alq_3)_2$-OT is the same as that of compound **5**. This demonstrates that the redox properties of $(Alq_3)_2$-OT originate from its components Alq_3 and compound **5**. The LUMO energy level of the compound **5** (-2.2 eV) is higher than that of Alq_3 (-2.4 eV). Therefore, it is reasonable that the intramolecular electron transfer in $(Alq_3)_2$-OT from the excited oligothiophene backbone to the charge transfer state (CTS) of the end-capped Alq_3 complexes occurs and it is a competing process with oligothiophene fluorescence relaxation. In addition, the maximum of $(Alq_3)_2$-OT excitation spectra blue shifts compared to its absorption maxima (see ESI, Figure S5) due to the intramolecular electron transfer.

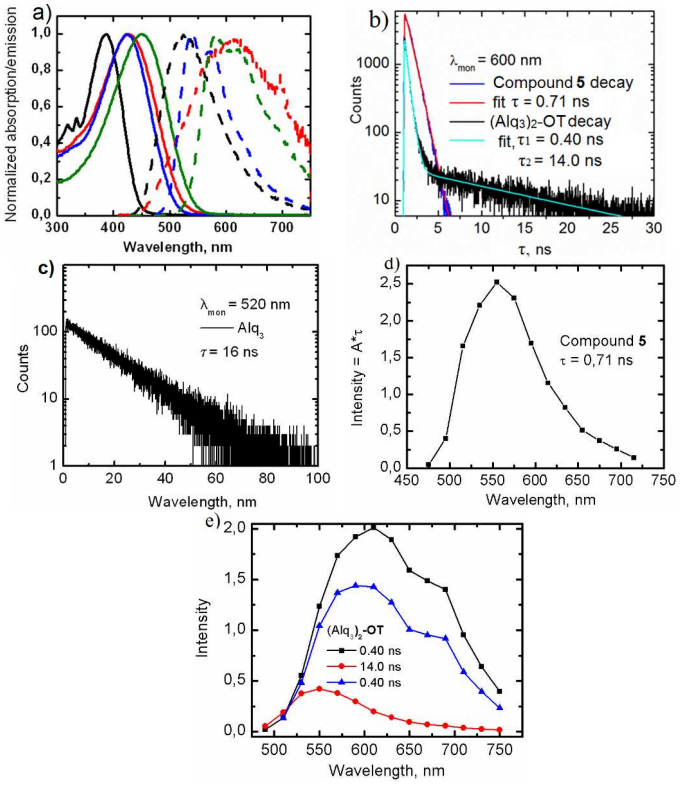

Figure 1. (a) Normalized absorption (solid lines) and emission (dashed lines) spectra of compound **5** (blue), $(Alq_3)_2$-OT (red), Alq_3 (black) and P3HT (green). **(b)** Fluorescence decay curves of compounds **5** and $(Alq_3)_2$-OT (λ_{ex} = 405 nm) **(c)** Fluorescence decay curve of Alq_3 (λ_{ex} = 405 nm). **(d)** Fluorescence DAS of compound **5** (λ_{ex} = 405 nm). **(e)** Fluorescence DAS of $(Alq_3)_2$-OT, (λ_{ex} = 405 nm: black and red curves, λ_{ex} = 483 nm: blue curve). All measured in $CHCl_3$.

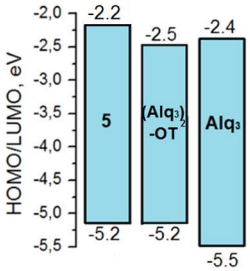

Figure 2. HOMO and LUMO energy levels of compound **5**, $(Alq_3)_2$-OT and Alq_3.[6a]

For TCSPC measurements of $(Alq_3)_2$-OT, the excitation wavelength of 483 nm was used to solely excite the oligothiophene backbone of the $(Alq_3)_2$-OT. As shown in Figure 1e, excitation at 483 nm results in only one component, similar to the short living component in the 405 nm excitation. Energy transfer from the oligothiophene backbone to the Alq_3 moieties can be excluded, because the 14 ns component does not exist when exciting at 483 nm.

The behaviour of the molecules in the presence of a quencher molecule, PCBM, was investigated in additional steady state measurements. The compounds were measured without PCBM and then immediately after with PCBM. Therefore, the intensities of the absorption and emission spectra are comparable. Absorption and emission spectra of compound **5**, $(Alq_3)_2$-OT and Alq_3 in the presence and absence of PCBM in $CHCl_3$ are shown in Figures 3a–b.

As the lifetimes of the oligothiophene backbones are 0.7 and 0.4 ns for compound **5** and $(Alq_3)_2$-OT, respectively, and the concentration of PCBM is as low as 0.84 mM, the 40–60 % decrease in the fluorescence intensities (Figure 3b) would not be possible by diffusion. Thus the observed quenching is due to static quenching (See also ESI, p. 17).

The films prepared from $(Alq_3)_2$-OT, PCBM and mixtures of the three different mass ratios, (Figure 3c) were studied using steady state emission (Figure 3d) and TCSPC methods. The emission of $(Alq_3)_2$-OT is quenched (Figure 3d) as a function of PCBM content in the solid films. The emission intensity also decreases in TCSPC measurements when the PCBM content is increased and same photon collection time is used (See ESI, Figure S1).

Because PCBM efficiently quenches the emission of $(Alq_3)_2$-OT, it seems that $(Alq_3)_2$-OT is able to donate an electron to PCBM. Therefore, to further study the intra- and intermolecular electron transfer, time resolved absorptions of $(Alq_3)_2$-OT in the presence and absence of PCBM were measured with a pump-probe set-up in chloroform. The transient absorption and decay component spectra are shown in Figure 4. The measurements were carried out until a 2000 ps delay, therefore the components with lifetimes longer than that are extrapolations and given as $\tau > 2000$ ps, the upper limit of the time-resolution of the instrument.

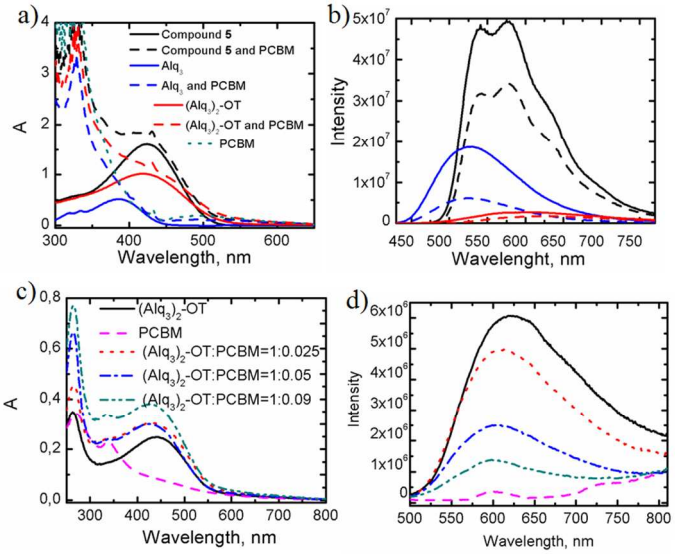

Figure 3. (a) Absorption and **(b)** emission spectra (λ_{ex} = 405 nm) of the compound **5** (0.22 mM), $(Alq_3)_2$-OT (0.22 mM), and Alq_3 (0.44 mM) in the absence (solid lines) and presence of PCBM (0.84 mM) (dashed lines) in $CHCl_3$. **(c)** Absorption and **(d)** emission (λ_{ex} = 405 nm) spectra of $(Alq_3)_2$-OT, PCBM and their mixtures of three different mass ratios in films.

Figure 4a, which presents the decay component spectra (blue, black, and red curves) and the transient absorption spectrum at delay time 0 ps (green curve) for $(Alq_3)_2$-OT, describes together with Figure 5a the processes following the photoexcitation. With the 390 nm excitation, both the oligothiophene backbone and Alq_3 moieties are excited. The first component (blue triangles), is formed very fast (<< 2 ps) indicated by negative bands at the wavelength areas, at which hexathiophene cation radical, around 800 nm[11], and Alq_3 anion radical, around 550 nm[12], have their absorptions. We describe this state as excited charge transfer complex (CTC), covering the positive bands from 600 to 1050 nm. CTC decays in 2 ps to an intramolecular charge transfer state (ICTS, black circles). The broad absorption of ICTS, 600 – 1000 nm, consists of the broadened and red shifted intramolecular absorptions of the Alq_3 anion (550 nm and longer) and hexathiophene cation radicals (800 nm and longer). The charge transfer state recombines to the ground states with lifetime of 250 ps. The third component with $\tau >$ 2000 ps (red squares) is associated to the broad and long-lived (τ = 14 ns by TCSPC) singlet excited state of the Alq_3 moiety.[13]

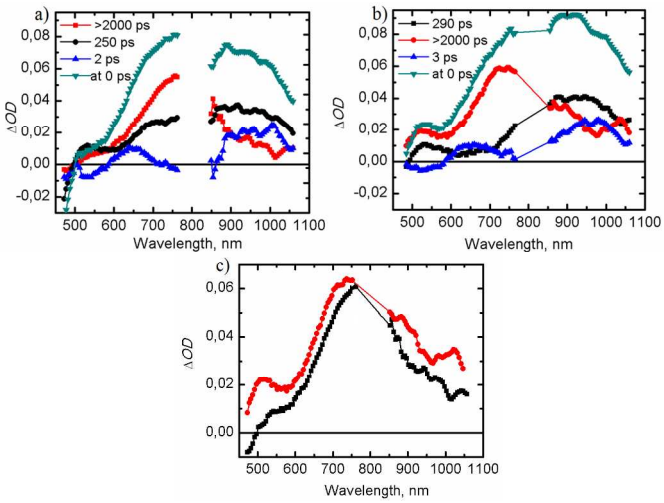

Figure 4. Decay component spectra and calculated transient spectrum at 0 ps delay time of $(Alq_3)_2$-OT (0.22 mM) **(a)** in the absence and **(b)** in the presence of PCBM. (**c**) Calculated transient absorption spectra of $(Alq_3)_2$-OT (0.22 mM) in the absence (black squares) and presence (red circles) of PCBM (0.84 mM) after 300 ps of the excitation (λ_{ex} = 390 nm).

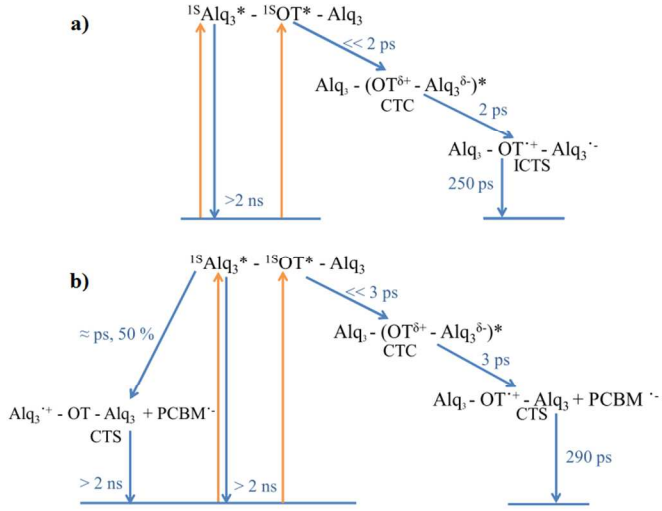

Figure 5. Reaction scheme of the phenomena in $(Alq_3)_2$-OT (blue arrows) after photoexcitation (yellow arrows) **(a)** in the absence and **(b)** in the presence of PCBM.

Mixing $(Alq_3)_2$-OT with PCBM causes changes both in the decay component spectra (Figures 4b and 5b) and in the time-resolved absorption spectra (Figure 4c and S4). The first component, 3 ps (blue triangles), corresponds the CTC state similar as in Figure 4a, in the absence of PCBM. The essential changes are observed in the second component, 290 ps (black squares), in which the short wavelength (600 nm – 750 nm) component of the absorption, corresponding to the Alq_3 anion radical band in Figure 4a, is absent. Evidently, PCBM has captured the electron from the formed ICTS and only the absorption of the hexathiophene cation radical is left. Its lifetime is increased, because the recombination with the counter anion radical is delayed. Instead it recombines with the PCBM radical anion in time of about 290 ps.

There are, however, PCBM anion radicals present after 300 ps (Figure 4b-c) and 1000 ps (Figure S4) after excitation, as indicated by the absorption bands at 1050 nm.[11] Thus there is another way for its formation. As can be seen from Figure 3b and Table 1, the fluorescence of Alq_3 moiety in $(Alq_3)_2$-OT was quenched about 40 % in the presence of PCBM. Thus an alternative path for formation of PCBM radical anion is the electron transfer from Alq_3 singlet excited state to PCBM. This can also be seen as Alq_3 cation radical band at 550 nm[12] in Figures 4b and c, as well as in Figure S4. The most probable reactions paths in the presence of PCBM are presented in Figure 5b.

Photovoltaic performance. Compounds **5**, $(Alq_3)_2$-OT and Alq_3 were applied as dopants in the photoactive BHJ layer of inverted ITO|ZnO|P3HT:PCBM|Alq_3|Au organic solar cells. The schematic structure of the cell and the chemical structures of the donor molecule P3HT, acceptor molecule PCBM, and buffer layer material Alq_3 are presented in Figure 6. The use of compound **5** as the dopant molecule decreased the cell efficiency when compared to the undoped reference cell (See ESI, Table S1). Instead, the best cell doped with $(Alq_3)_2$-OT had an efficiency of 2.63 %, which is higher than that of the reference cell (Table 2). After a four week storage period, efficiencies of all doped devices were better than that of the reference cell. Moreover, the efficiency of the best cell doped with $(Alq_3)_2$-OT had increased to 2.85 %, which demonstrates high stability of cells doped with $(Alq_3)_2$-OT.

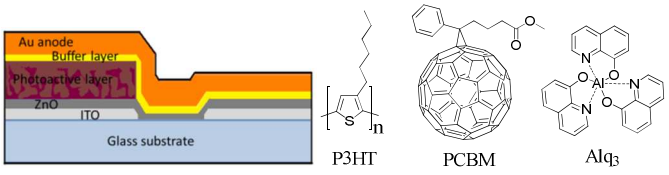

Figure 6. Structure of the inverted solar cell and chemical structures of P3HT donor, PCBM acceptor and Alq_3 buffer layer material.

The effect of doping with large concentrations of free Alq_3 complex and the equivalent amount of Alq_3 bound to the oligothiophene backbone in $(Alq_3)_2$-OT was compared in solar cells. As shown in Table 3, the use of a relatively high content of free Alq_3 dopant decreases *FF* and cell efficiency compared to cells doped with equivalent amounts of the complexes bound to $(Alq_3)_2$-OT or without doping. The cell containing $(Alq_3)_2$-OT as a dopant showed highest J_{sc}, V_{oc}, and efficiency. The results clearly demonstrate that the oligothiophene backbone of $(Alq_3)_2$-OT increases the compatibility of Alq_3 with the P3HT:PCBM blend, and $(Alq_3)_2$-OT can be inserted in the BHJ layer as a third component without destroying the layer morphology.

Table 2. Photovoltaic parameters of the cells doped with $(Alq_3)_2$-OT.

c($(Alq_3)_2$-OT)* (mM)	Storage time	$J_{sc,best}$ (mA/cm^2)	$V_{oc,best}$ (V)	FF_{best} (%)	η_{best} (%)	η_{avg} (%)
0	1 day	-2.86	0.50	59	2.33	**2.06**
0.15	"	-2.97	0.52	61	**2.63**	**2.50**
0.60	"	-3.04	0.52	60	2.62	**2.31**
0.90	"	-2.52	0.53	55	2.07	**1.90**
0	4 weeks	-2.74	0.53	57	2.31	**2.06**
0.15	"	-2.99	0.55	62	**2.85**	**2.55**
0.60	"	-2.66	0.56	60	2.49	**2.22**
0.90	"	-2.59	0.55	60	2.36	**2.13**

*Concentration of $(Alq_3)_2$-OT in the spin-coated P3HT:PCBM solution

Table 3. Photovoltaic parameters of the cells doped with $(Alq_3)_2$-OT and Alq_3.

Dopant	c_{dopant} (mM)	$J_{sc,best}$ (mA/cm^2)	$V_{oc,best}$ (V)	FF_{best} (%)	η_{best} (%)	η_{avg} (%)
-	-	-2.67	0.53	63	2.51	**2.33**
$(Alq_3)_2$-OT	0.57	-2.84	0.56	60	2.69	**2.40**
$Alq_3$1.14	1.14	-2.74	0.51	49	2.41	**2.12**

The use $(Alq_3)_2$-OT as a buffer layer was also investigated. $(Alq_3)_2$-OT was thermally vacuum evaporated (185–285 °C) between the photoactive layer and Au anode. Absorption and emission spectra of the evaporated films and the differential scanning calorimetry (DSC) curve of $(Alq_3)_2$-OT are shown in the ESI (S2 and S3). $(Alq_3)_2$-OT is thermally stable until 400 °C based on the DSC measurement.

The cell parameters were measured one day and four weeks after the cell preparation (Table 4). Meanwhile, the cells were stored in the dark and the ambient atmosphere. The cells with the parent Alq_3 as a buffer layer showed a slight decrease in current and efficiency over the time, whereas the cells equipped with $(Alq_3)_2$-OT as a buffer layer showed improved cell parameters.

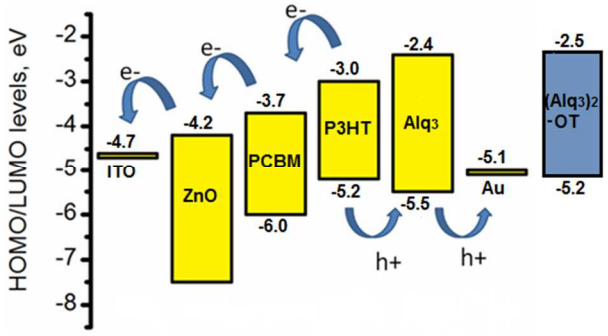

Figure 7. Energy levels[14,6] of the solar cell structure and HOMO and LUMO levels of $(Alq_3)_2$-OT.

Based on the results, it is evident that the used cell structure has a relatively high shelf-lifetime and that $(Alq_3)_2$-OT seems to function better as a hole transporting buffer layer than Alq_3. Also, the remarkable decrease in the series resistance (R_s) implies that $(Alq_3)_2$-OT decreases the intrinsic resistance of the cell when compared to Alq_3.[15]

Energy levels of $(Alq_3)_2$-OT are suitably aligned with those of the other materials used in the cell. The HOMO and LUMO levels of $(Alq_3)_2$-OT are shown together with the energy levels of the inverted cell structure in Figure 7. The 0.3 eV higher HOMO level of $(Alq_3)_2$-OT compared to that Alq_3 produces smaller extraction barrier for the photogenerated holes to escape the device[6b] when $(Alq_3)_2$-OT is used as a buffer material instead of Alq_3. This may explain the observed reduction of R_s values of the cells with $(Alq_3)_2$-OT as a hole transporting buffer material compared to cells with an Alq_3 buffer layer (Table 4).

The cell absorption spectra in Figure 8 show that the absorption of the cells is increased in the area around 400 nm, where the absorption of $(Alq_3)_2$-OT takes place. Therefore, more photons are absorbed when $(Alq_3)_2$-OT is used as a dopant. LUMO levels of $(Alq_3)_2$-OT and Alq_3 are nearly the same and higher than the LUMO of PCBM. Therefore, they can donate electron to PCBM. Because $(Alq_3)_2$-OT is capable of donating electrons to PCBM, as shown also by spectroscopic studies, it functions as an additional light-absorber and donates electrons to PCBM which increases the current of the cells. Also, some increase in the cell absorption can be seen as shoulders around 550 nm and 600 nm. This is possibly caused by the improved crystallinity of P3HT due to the inserted dopant molecules, which further supports the high compatibility of $(Alq_3)_2$-OT in the BHJ layer.

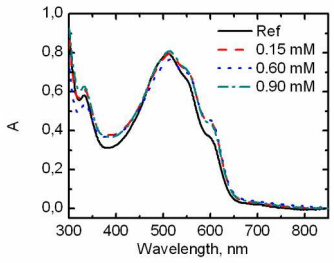

Figure 8. Absorption spectra of the reference cell without doping and cells with $(Alq_3)_2$-OT as a dopant in the BHJ layer.

Table 4. Photovoltaic parameters and resistances of the cells with Alq_3 or $(Alq_3)_2$-OT as buffer layers.

Buffer layer (thickness)	Storage time	$J_{sc,\,best}$ (mA/cm^2)	$V_{oc,best}$ (V)	FF_{best} (%)	η_{best} (%)	η_{avg} (%)	R_s (Ω cm^2)	R_{sh} (Ω cm^2)
Alq_3 (~5 nm)	One day	-2.62	0.55	60.	**2.42**	2.25	39.64	1499
$(Alq_3)_2$-OT (~6.5 nm)	"	-2.71	0.50	58	**2.18**	1.93	28.72	1385
$(Alq_3)_2$-OT (~9 nm)	"	-2.84	0.46	54.76	**1.99**	1.86	29.19	931.1
Alq_3 (~5 nm)	4 weeks	-2.54	0.54	61	**2.33**	2.05	45.12	1998
$(Alq_3)_2$-OT (~6.5 nm)	"	-2.85	0.53	58	**2.45**	2.22	29.62	1310
$(Alq_3)_2$-OT (~9 nm)	"	-3.11	0.51	56	**2.47**	2.06	33.43	1494
Alq_3 (~5 nm)	12 weeks	-2.32	0.55	61	**2.28**	2.03	46.20	2098
$(Alq_3)_2$-OT (~6.5 nm)	"	-2.76	0.52	61	**2.54**	2.10	29.44	1545
$(Alq_3)_2$-OT (~9 nm)	"	-2.81	0.54	56	**2.45**	2.13	35.84	2453

Conclusion

Detailed understanding of inter- and intramolecular properties and molecular interactions is a prerequisite for developing new photoactive and functional materials with desired properties. We synthesized an Alq_3 end-capped oligothiophene, $(Alq_3)_2$-OT, and concentrated on understanding its photophysical properties utilizing steady state and time resolved optical spectroscopic methods. When $(Alq_3)_2$-OT was photoexcited an intramolecular electron transfer from the oligothiophene backbone to the Alq_3 moiety was observed. In the presence of PCBM $(Alq_3)_2$-OT donates electron to PCBM. After these observations $(Alq_3)_2$-OT was applied as a dopant molecule in the P3HT:PCBM active layer of BHJ based organic solar cell, which increased the cell efficiency. Previous reports suggested that the cell efficiency is increased due to improved morphology of the BHJ photoactive layer caused by doping. The current studies strongly support the idea that $(Alq_3)_2$-OT can also function in the BHJ active layer as an additional light-absorber which donates electrons to PCBM and improves the cell efficiency. Moreover, the suitable energy levels allow the use of $(Alq_3)_2$-OT as an interfacial layer between the active layer and gold anode improving the cell performance and shelf-lifetime. These findings provide new insights useful in designing more effective photoactive materials for photovoltaic applications.

Experimental section

Synthesis of the compounds. (8-(benzyloxy)-5-(4,4,5,5-tetramethyl-1,3,2-dioxaborolan-2-yl)quinolone) and 8-(benzyloxy)-5-bromoquinoline were synthesized using previously published methods.[16]

Compound 2. Commercial starting material **1** (200 mg, 0.40 mmol), NBS (151 mg, 0.85 mmol) and ethyl acetate (7 mL) were placed in a reaction flask. The reaction mixture was irradiated by ultrasound for 1 h.[17] The solvent was evaporated and the product was purified by flash-chromatography (SiO_2, *n*-hexane). Compound **2** was collected as yellow powder (239 mg, 91%). ^{1}H NMR ($CDCl_3$, 300 MHz): δ ppm 0.89 (t, J = 6.60 Hz, 6H), 1.28–1.42 (m, 12H), 1.59–1.67 (m, 4H), 2.72 (t, J = 7.50 Hz, 4H), 6.91 (s, 2H), 6.97 (d, J = 3.93 Hz, 2H), 7.12 (d, J = 3.93 Hz, 2H).

Compound 3. Compound **2** (201 mg, 0.31 mmol), toluene (9 mL), ethanol (3 mL) and distilled water (3 mL) were bubbled with argon for 15 min. K_2CO_3 (181 mg, 1.31 mmol), $Pd(PPh_3)_4$ (44.8 mg, 0.039 mmol) and 3-hexylthiophene-2-boronic acid pinacol ester (0.20 mL, 0.63 mmol) were added and the reaction mixture was refluxed under argon for 5 h. The solvents were evaporated and ethyl acetate (20 mL) was added. The solution was extracted two times with distilled water (6 mL) and the organic layer was dried with $MgSO_4$. The solution was filtered and evaporated to dryness. Flash-chromatography (SiO_2, *n*-hexane) afforded the compound **3** as a yellow reddish oil (246 mg, 97%). ^{1}H NMR ($CDCl_3$, 300 MHz): δ ppm 0.89–0.94 (m, 12H), 1.30–1.45 (m, 24H), 1.62–1.76 (m, 8H), 2.78–2.83 (m, 8H), 6.95 (d, J = 5.20 Hz, 2H), 6.97 (s, 2H), 7.07 (d, J = 3.74 Hz, 2H), 7.16 (d, J = 3.74 Hz, 2H), 7.18 (d, J = 5.20 Hz, 2H).

Compound 4. Compound **4** was prepared using the same method as compound **2**. The specific amounts of chemicals used: compound **3** (170 mg, 0.20 mmol), NBS (76.9 mg, 0.43 mmol) and 4 mL ethyl acetate. Flash-chromatography (SiO_2, *n*-hexane) afforded the compound **4** as a red powder (180 mg, 89%). ^{1}H NMR ($CDCl_3$, 300 MHz): δ ppm 0.88–0.93 (m, 12H), 1.30–1.40 (m, 24H), 1.57–1.73 (m, 8H), 2.70–2.81 (m, 8H), 6.90 (br. s, 4H), 7.05 (d, J = 3.74 Hz, 2H), 7.15 (d, J = 3.74 Hz, 2H).

Compound 5. Method A: Suzuki-Miyaura coupling. Toluene (4.5 mL), ethanol (1.5 mL) and distilled water (1.5 mL) were bubbled with argon for 15 min. Compound **4** (150 mg, 0.15 mmol), 8-(benzyloxy)-5-(4,4,5,5-tetramethyl-1,3,2-dioxaborolan-2-yl)quinoline (109 mg, 0.30 mmol), K_2CO_3 (93.7 mg, 0.68 mmol) and $Pd(PPh_3)_4$ (21.3 mg, 0.018 mmol) were added and the reaction mixture was refluxed under argon for 5 h. The solvents were evaporated and the crude product was dissolved in toluene (15 mL). The solution was transferred to a flash-chromatography column (SiO_2) and eluated with the

mixture of EtOAc/*n*-hexane (2:1). The solid crude product obtained from column purification was stirred with acetone (3 mL), filtered and washed with acetone (9 mL). The procedure afforded the compound **5** as an orange powder (167 mg, 85 %). Method B: direct arylation. Compound **3** (246 mg, 0.30 mmol) was dissolved in DMA (3 mL). The solution was bubbled with argon for 15 min. K_2CO_3 (206 mg, 1.50 mmol), $Pd(OAc)_2$ (6.8 mg, 0.03 mmol), $PCy_3{\cdot}HBF_4$ (22.7 mg, 0.06 mmol), pivalic acid (19.4 mg, 0.19 mmol) and 8-(benzyloxy)-5-bromoquinoline (187 mg, 0.60 mmol) were added and the reaction mixture was heated (150 °C) under argon for 24 h. The reaction mixture was filtered through a thin pad of silica gel, the filter washed with chloroform, (ca. 20 mL) and the solvents evaporated. The crude product was stirred with acetone (3 mL), filtered and washed with acetone (10 mL) and ethanol (5 mL). The procedure afforded the compound **5** as orange powder (334 mg, 87 %). ^{1}H NMR ($CDCl_3$, 300 MHz): δ ppm 0.89–0.94 (m, 12H),1.34–1.45 (m, 24H), 1.66–1.78 (m, 8H), 2.79–2.88 (m, 8H), 5.51 (s, 4H), 6.98 (s, 2H), 7.01 (s, 2H), 7.05–7.09 (m, 4H), 7.17 (d, J = 3.74 Hz, 2H), 7.32–7.42 (m, 6 H), 7.48–7.56 (m, 8H), 8.64 (dd, J = 8.56, 1.71 Hz, 2H), 9.03 (dd, J = 4.20, 1.71 Hz, 2H). ^{13}C NMR ($CDCl_3$, 75 MHz): δ ppm 14.1, 22.6, 22.6, 29.2, 29.3, 29.4, 29.5, 30.5, 30.6, 31.7, 70.7, 109.3, 121.9, 123.9, 124.3, 126.3, 127.0, 127.8, 127.9, 128.2, 128.6, 128.7, 130.2, 130.3, 130.8, 134.0, 134.1, 135.0, 136.7, 136.7, 138.5, 140.0, 140.1, 140.5, 149.4, 154.2. HRMS: calcd for $C_{80}H_{84}N_2O_2S_6Na$ ([M + Na]$^+$) 1319.4755, found 1319.4812.

Compound 6. Compound **5** (100 mg, 0.077 mmol) was dissolved in CH_2Cl_2 (7.5 mL). The reaction system was charged with argon and cooled on ice bath. A 1M BBr_3 in CH_2Cl_2 solution (1.6 mL, 1.60 mmol) was slowly added.The reaction mixture was stirred at room temperature overnight. The reaction mixture was cooled on ice bath and saturated $NaHCO_3$(aq) (8 mL) was slowly added. The mixture was evaporated to dryness. Toluene (15 mL) and distilled water (5 mL) were added. The organic layer was dried with Na_2SO_4 and filtered. The filter was washed with a small amount of chloroform and the filtrate was evaporated to dryness. The crude product was stirred with acetone (1.5 mL), filtered and washed with acetone (6.5 mL). The procedure afforded the compound **6** as dark red powder (65.0 mg, 75%). ^{1}H NMR ($CDCl_3$, 300 MHz): δ ppm 0.89–0.94 (m, 12H), 1.35–1.47 (m, 24H), 1.67–1.77 (m, 8H), 2.80–2.89 (m, 8H), 7.01 (s, 2H), 7.03 (s, 2H), 7.09 (d, J= 3.74 Hz, 2H), 7.18 (d, J = 3.74 Hz, 2H), 7.22 (d, J = 7.90 Hz, 2H), 7.52 (dd, J = 8.60, 4.20 Hz, 2H), 7.61 (d, J = 7.90 Hz, 2H), 8.68 (dd, J = 8.60, 1.56 Hz, 2H), 8.83 (dd, J = 4.20, 1.56 Hz, 2H). ^{13}C NMR ($CDCl_3$, 50 MHz): δ ppm 14.1, 22.6,22.7, 29.2, 29.3, 29.5, 29.6, 29.7, 30.5, 30.7, 31.7, 109.5, 122.2,122.7, 123.9, 126.3, 126.8, 128.7, 129.3, 130.0, 130.2, 130.7, 134.0, 134.6, 135.0, 136.7, 138.3, 138.6, 140.0, 140.1, 147.9, 152.3. HRMS: calcd for $C_{66}H_{73}N_2O_2S_6$ ([M + H]$^+$) 1117.3996, found 1117.3999.

$(Alq_3)_2$-OT. Compound **6** (20.0 mg, 0.018 mmol), 8-hydroxyquinoline (10.4 mg, 0.072 mmol), Al(i-PrO)$_3$ (7.3 mg, 0.036 mmol), $CHCl_3$ (2 mL) and ethanol (1 mL) were placed in a reaction flask which was charged with argon. The reaction mixture was stirred and refluxed for 17 h. The solvents were evaporated and methanol (5 mL) was added. The precipitate was filtered and washed with acetone (10 mL). The procedure afforded the $(Alq_3)_2$-OT as orange powder (29.3 mg, 94 %). ^{1}H NMR ($CDCl_3$, 300 MHz): δ ppm 0.91 (br. s., 12H), 1.33–1.42 (m, 24H), 1.71 (br. s., 8H), 2.78–2.86 (m, 8H), 6.92–6.99 (m, 5H), 7.07–7.17 (m, 13H), 7.34–7.54 (m, 11H), 7.62–7.66 (m, 3H), 8.24–8.32 (m, 4H), 8.76–8.94 (m, 6H). HRMS: calcd for $C_{102}H_{95}N_6O_6Al_2S_6$ ([M + H]$^+$) 1745.5268, found 1745.5266.

$(Alq_3)_2$-OT and PCBM film preparation. All film samples were prepared on quartz plates. The PCBM film was spin-coated for 5 mins (600 rpm) from a 14.1 mg/ml DCB solution. The film of $(Alq_3)_2$-OT was drop-cast from 400 µl of 0.40 mg/ml $(Alq_3)_2$-OT chloroform solution. The film of $(Alq_3)_2$-OT with 2.5 m-% PCBM was drop cast from 400 µl of a mixed 0.40 mg/ml $(Alq_3)_2$-OT and 0.01 mg/ml PCBM chloroform solution. The film of $(Alq_3)_2$-OT with 5 m-% PCBM was drop cast from 400 µl of a mixed 0.40 mg/ml $(Alq_3)_2$-OT and 0.02 mg/ml PCBM chloroform solution. The film of $(Alq_3)_2$-OT with 9 m-% of PCBM was drop cast from a 0.40 mg/ml $(Alq_3)_2$-OT and 0.04 mg/ml PCBM chloroform solution.

Spectroscopic measurements. The steady state absorption and fluorescence were measured employing a UV-3600 Shimadzu UV-VIS-NIR spectrophotometer and a Jobin Yvon-SPEX fluorolog. The fluorescence lifetimes were measured using a time correlated single photon counting (TCSPC) system equipped with a Picoharp 300 controller and a PDL 800-B driver for excitation and a microchannel plate photomultiplier (Hamamatsu R3809U-50) for detection in 90º configuration. The excitation wavelengths were 405 nm and 483 nm and pulse frequency 2.5 MHz. Pump-probe technique for time resolved absorption was used to detect the fast processes with a time resolution shorter than 0.2 ps. The instrument and the used data analysis procedure have been reported earlier.[18]

Solar cell preparation. The solvents and Alq_3 (99.995 %) were purchased from Sigma-Aldrich and used without further purification. The solar cell samples were prepared on ITO coated glass substrates (1.2 cm × 3.5 cm) purchased from Solems. The zinc-acetate ($Zn(OCOCH_3)_2{\cdot}2H_2O$) for ZnO layer preparation was purchased from Sigma-Aldrich. Reference polymer, P3HT, was purchased from Rieke Metals and acceptor $PC_{60}BM$ (99.0 %) from Nano-C.

Solar cells were constructed on commercial ITO covered glass substrates. The ITO layer was taped and lacquered for *aqua regia* etching to achieve a patterned ITO. The etched plates were cleaned by sonicating in acetone, chloroform, SDS solution (20 mg sodium dodecyl sulphate in 500 mL Milli-Q H_2O), Milli-Q H_2O and 2-propanol (30 min in each), in the previously stated order, and dried under vacuum at 150 ºC for one hour. After a 10 min N_2 plasma cleaning procedure (Harrick Plasma Cleaner PDG-236), a 20 nm ZnO layer was deposited by 1 min spin-coating in WS-400B-6NPP/LITE spin-coater from Laurell Technologies from 50 g L^{-1} zinc-acetate in 96 % 2-methoxyethanol and 4 % ethanolamine solution following the literature process.[19]

The photoactive layer compounds, P3HT, $PC_{60}BM$ and dopant, were dissolved in 1,2-dichlorobenzene:chloroform (2:1

V-%) mixture and stirred (250 rpm) overnight at 50 ºC. Spin-coating of the BHJ photoactive layer from the P3HT:PCBM:dopant blend took 5 minutes (600 rpm) in the spin-coater under N_2 flow. The spin-coated films were annealed under vacuum at 110 ºC for 10 min. Buffer layer and Au anode were evaporated in the vacuum evaporator under ~ 3×10^{-6} mbar pressure. The evaporation rate and film thickness were controlled with evaporator crystals to deposit the desired thickness of the buffer and ~50 nm thick Au anode layers on top of the photoactive layer. The cells were stored in the ambient atmosphere in the dark before measurements and analysis.

The photovoltaic parameters were obtained and calculated from current-voltage (*I-V*) curves, which were measured in the dark and under simulated AM 1.5 sunlight illumination (50 mW cm^{-2}) using an Agilent E5272A source/monitoring unit. A voltage of -0.20 V – 0.60 V was applied in 10 mV steps. The measurements were carried out in ambient atmosphere at room temperature without encapsulation of the devices. The illumination was produced by a filtered Xe-lamp (Oriel Corporation & Lasertek) in the Zuzchem LZC-SSL solar simulator. The illumination power density was measured using a Coherent Fieldmax II LM10 power meter. Because a certified measuring system could not be employed, the absolute efficiency values are not directly comparable with the other published results. However, the reported efficiencies and the relative efficiency changes are comparable within the presented devices.

To determine the thickness the evaporated buffer layers, reference quartz plates were placed into the evaporator chamber for each buffer evaporation. A narrow strip of the reference film was removed with a cotton stick dipped in $CHCl_3$ and the step was measured with a Veeco Wyko NT-1100 profilometer. The profilometer data were recorded from (230×300) μm^2 and analyzed by phase shift interferometry (PSI) mode. The vertical resolution of this method is close to 1 Å according to the instrument manual and the horizontal resolution of the objective ($20 \times$ magnification) is 0.75 μm.

Electrochemical measurements. Differential pulse voltammetry (DPV) measurements were carried out by employing an Iviumstat (Compactstat IEC 61326 Standard) potentiostat and a three-electrode cell configuration to determine HOMO and LUMO energy levels for compound **5** and $(Alq_3)_2$-OT**.** The measurements were carried out using 0.1 M $TBAPF_6$ in dichloromethane (DCM) as supporting electrolyte, glass platinum electrode as working electrode, graphite rod as counter electrode and platinum wire as pseudo reference electrode. For each sample, the background was measured for 2.5 ml of the electrolyte solution after 20 min deoxygenation purging N_2. 100 μl of 0.5 mM sample in DCM was inserted and the system was stabilized again purging N_2. Each sample was measured between -2.5 V and 2.0 V scanning in both directions with 2.5 mV steps. Ferrocene (Acros Organics, 98%) was used as internal standard reference to scale the measured potentials against vacuum level[20]. HOMO and LUMO level calculations were based on the formal oxidation and reduction potentials observed in the DPV curves according to the following equations:

$$E_{HOMO} = -(4.8 + E_{dif,ox})eV$$
$$E_{LUMO} = (-E_{dif,red} + 4.8)eV$$

where 4.8 eV is the oxidation energy of ferrocene. $E_{dif,ox}$ is the difference in volts between the formal oxidation potentials of ferrocene and the measured sample. $E_{dif,red}$ is the difference in volts between the formal oxidation potential of ferrocene and the formal reduction potential of the sample. See the HOMO and LUMO level calculations in ESI p. 19 – 20.

Author contributions

O.E.O.H. and H.J.L. act as group leaders. J.P.H. synthesized and characterized all the compounds. V.M.M. carried out spectroscopic and electrochemical studies and solar cell experiments. K.M.K. helped with the fittings and analysis of the pump-probe measurements. All authors took part in the writing of the manuscript.

Acknowledgements

The National Doctoral Programme in Nanoscience (NGS-NANO) is greatly acknowledged for funding. Tero-Petri Ruoko is acknowledged for helping with the pump-probe measurements.

Notes and references

[a]Department of Chemistry and Bioengineering, Tampere University of Technology, P.O. Box 541, FI-33101, Tampere, Finland.
[b]Department of Chemistry, University of Oulu, P.O. Box 3000, FI-90014, Finland.

Electronic Supplementary Information (ESI) available: ^{1}H NMR spectra of compounds **2**–**4**, ^{1}H and ^{13}C NMR spectra of compounds **5** and **6**, ^{1}H NMR spectrum of $(Alq_3)_2$-OT, Quenching of compound **5**, Alq_3 and $(Alq_3)_2$-OT and in the presence of PCBM, TCSPC decay curves of the $(Alq_3)_2$-OT and PCBM film samples and DAS spectra of $(Alq_3)_2$-OT and PCBM in $CHCl_3$, Table of the solar cell results with compound **5**, Absorption and emission spectra of the evaporated films of $(Alq_3)_2$-OT, DSC curve of $(Alq_3)_2$-OT, Transient absorption and decay component spectra of the $(Alq_3)_2$-OT mixed with PCBM, DPV curves of $(Alq_3)_2$-OT and compound **5**, See DOI: 10.1039/b000000x/.

[1](a) B. Walker, A. B. Tamayo, X.-D. Dang, P. Zalar, J. H. Seo, A. Garcia, M. Tantiwiwat and T.-Q. Nguyen, *Adv. Funct. Mater.,* 2009, **19**, 3063. (b) A. B. Tamayo, X.-D. Dang, B. Walker, J. Seo, T. Kent

and T.-Q. Nguyen, *Appl. Phys. Lett.,* 2009, **94**, 103301. (c) M. S. Wrackmeyer, M. Hein, A. Petrich, J. Meiss, M. Hummert, M. K. Riede and K. Leo, *Sol. Energy Mater. Sol. Cells*, 2011, **95**, 3171. (d) R. Fitzner, C. Elschner, M. Weil, C. Uhrich, C. Körner, M. Riede, K. Leo, M. Pfeiffer, E. Reinold, E. Mena-Osteritz and P. Bäuerle, *Adv. Mater.,* 2012, **24**, 675

[2]Y. Ooyama and Y. Harima, *Eur. J. Org. Chem.,* 2009, 2903.

[3]C. W. Tang and S. A. VanSlyke, *Appl. Phys. Lett.,* 1987, **51**, 913.

[4](a) A. Fuchs, D. Steinbrecher, M. S. Mommer, Y. Nagata, M. Elstner and C. Lennarts, *Phys. Chem. Chem. Phys.*, 2012, **14**, 4259. (b) S. Barth, P. Müller, H. Riel, P.F. Seidler, W. Riess, H. Vestweber and H. Bässler, *J. Appl. Phys.* 2001, **89**, 3711.

[5]Q. L. Song, F. Y. Li, H. Yang, H. R. Wu, X. Z. Wang, W. Zhou, J. M. Zhao, X. M. Ding, C. H. Huang and X. Y. Hou, *Chem. Phys. Lett.,* 2005, **416**, 42.

[6](a) A.Tolkki, K. Kaunisto, J. P. Heiskanen, W. A. E. Omar, K. Huttunen, S. Lehtimäki, O. E. O. Hormi and H. Lemmetyinen, *Thin Solid Films*, 2012, **520**, 4475. (b) V. M. Manninen, W. A. E. Omar, J. P. Heiskanen, H. Lemmetyinen and O. E. O. Hormi, *J. Mater. Chem*., 2012, **22**, 22971.

[7](a) H. Kanato, K. Takimiya, T. Otsubo, Y. Aso, T. Nakamura, Y. Araki and O. Ito, *J. Org. Chem.,* 2004, **69**, 7183. (b) N. Kiriy, A. Kiriy, V. Bocharova, M. Stamm, S. Richter, M. Plötner, W.-J. Fischer, F. C. Krebs, I. Senkovska and H.-J. Adler, *Chem. Mater.,* 2004, **16**, 4757. (c) C.-H. Chen, K.-Y. Liu, S. Sudhakar, T.-S. Lim, W. Fann, C.-P. Hsu and T.-Y. Luh, *J. Phys. Chem. B*, 2005, **109**, 17887. (d) A. Saeki, T. Fukumatsu and S. Seki, *Macromolecules*, 2011, **44**, 3416. (e) R. Stalder, D. Xie, R. Zhou, J. Xue, J. R. Reynolds and K. S. Schanze, *Chem. Mater.,* 2012, **24**, 3143.

[8]P. Arsenyan, E. Paegle and S. Belyakov, *Tetrahedron Lett.,* 2010, **51**, 205.

[9](a) G. D. Zhu, D.-H. Chen, J.-H. Huang and C.-S. Chi, *J. Org. Chem.,* 1992, **57**, 2316. (b) M. V. Adhikari and S. D. Samant, *Ultrason. Sonochem.,* 2002, **9**, 107. (c) G. A. Heropoulos, G. Cravotto, C. G. Screttas and B. R. Steele, *Tetrahedron Lett.,* 2007, **48**, 3247.

[10](a) D. J. Schipper and K. Fagnou, *Chem. Mater.,* 2011, **23**, 1594. (b) C. B. Bheeter, J. K. Bera and H. Doucet, *RSC Adv.,* 2012, **2**, 7197. (c) F. Derridj, K. S. Larbi, J. Roger, S. Djebbar and H. Doucet. *Tetrahedron,* 2012, **68**, 7463. (d) S. Bensaid and H. Doucet, *Tetrahedron*, 2012, **68**, 7655. (e) H. Zhao, C. Y. Liu, S. C. Luo, B. Zhu, T.-H. Wang, H.-F. Hsu and H.-H. Yu, *Macromolecules*, 2012, **45**, 7783. (f) K. Yamazaki, J. Kuwabara and T. Kanbara, *Macromol. Rapid Commun.,* 2013, **34**, 69. (g) G. Trippé-Allard and J.-C. Lacroix, *Tetrahedron*, 2013, **69**, 861.

[11]R. A. J. Janssen, M. P. T. Christiaans, K. Pakbaz, D. Moses, J. C. Hummelen and N. S. Saricifti, *J. Chem. Phys.* 1995, **102** , 2628.

[12]C. Ganzorig and M. Fujihira, *Appl. Phys. Lett.* 2002, **81**, 3137.

[13](a) S. Watanabe, A. Furube and R. Katoh, *J. Phys. Chem.A*, 2006, **110**, 10173. (b) S. Watanabe, M. Murai, Y. Tamaki, A. Furube and R. Katoh, Prog. *Int. Symp. Super-Functionality Organic Devises: IPAP Conf. Series* 6, 2005, pp. 121.

[14](a) HOMO and LUMO levels of P3HT and $PC_{60}BM$: A. K. K. Kyaw et al, Appl. Phys. Lett., 2008, **93**, 221107. (b) Energy levels of ZnO: S. S. Zade et al, *Acc. Chem. Res.* 2011, **44**, 14.

[15]Kim, M.-S.; Kim, B.-G.; Kim, J., *ACS Appl. Mater. Interfaces* 2009, **1**, 1264.

[16]V. A. Montes, R. Pohl, J. Shinar and P. Anzenbacher Jr., *Chem. Eur. J.,* 2006, **12**, 4523.

[17]Branson 2510 ultrasonic bath was used as an irradiation source.

[18]N. V. Tkachenko, L. Rantala, A. Y. Tauber, J. Helaja, P. H. Hynninen and H. J. Lemmetyinen, *J. Am. Chem. Soc.*, 1999, **121**, 9378.

[19]M. S. White, D. C. Olson, S. E. Shaheen, N. Kopidakis and D. S. Ginley, *Appl. Phys. Lett*., 2006, **89**, 143517.

[20] R. R. Gagne, C. A. Koval, G. C. Lisensky, *Inorg. Chem.* 1980, **19**, 2854.

